RESEARCH PAPER

A High Performance Electrochemical Sensor for Sulfite Based on $MOWS_2$ Nanocomposite Modified Electrode

Mohammad Reza Aflatoonian [1,2], Somayeh Tajik [1,3] *, Hadi Beitollahi [4] *, Somayeh Mohammadi [4], and Peyman Mohammadzadeh Jahani [5]

[1] *Research Center for Tropical and Infectious Diseases, Kerman University of Medical Sciences, Kerman, Iran*

[2] *Leishmaniasis Research Center, Kerman University of Medical Sciences, Kerman, Iran*

[3] *Neuroscience Research Center, Kerman University of Medical Sciences, Kerman, Iran*

[4] *Environment Department, Institute of Science and High Technology and Environmental Sciences, Graduate University of Advanced Technology, Kerman, Iran*

[5] *School of Medicine, Bam University of Medical Sciences ,Bam ,Iran*

ARTICLE INFO

Article History:
Received 14 November 2019
Accepted 06 January 2020
Published 01 April 2020

Keywords:
Graphite screen printed electrodes
$MOWS_2$ nanocomposite
Sensor
Sulfite

ABSTRACT

The present study reports synthesis of $MOWS_2$ nanocomposite followed by its characterization using energy dispersive X-ray spectroscopy (EDS), X-Ray diffraction (XRD) and field emission scanning electron microscopy (FESEM). Chronoamperometry (CHA), differential pulse voltammetry (DPV), and cyclic voltammetry (CV) have been used to examine electro-chemical behaviors of sulfite on $MOWS_2$ nanocomposite modified SPE. Electro-chemical specification indicated very good electro-catalytic activities and surface area impact of $MOWS_2$ nanocomposite. Oxidation signals of sulfite on $MOWS_2$/SPE has been considerably increased in comparison to the bare SPE. Within optimum conditions, quantification of sulfite might range between 0.08 to 700.0 μM with a small determination limit of 0.02 μM based on S/N=3.The impact of scan rates has been explored. Finally, the $MOWS_2$/SPE has been employed for detection of sulfite in real specimens. In general, an easy experimental method for manufacturing $MOWS_2$ nanocomposite has been suggested that takes advantage of selectivity, reproducibility, and sensitivity toward electro-active specimens, as well as biological matrices.

How to cite this article
Aflatoonian M, Tajik S, Beitollahi H, Mohammadi S, Mohammadzadeh Jahani P. A High Performance Electrochemical Sensor for Sulfite Based on $MOWS_2$ Nanocomposite Modified Electrode. J Nanostruct, 2020; 10(2):337-347. DOI: 10.22052/JNS.2020.02.013

INTRODUCTION

For many years, sulfite (SO_3^{2-}) has had a global widespread usage as a kind of food additives as sulfite, bisulfite, sulfur dioxide, and metabisulfite. It has been widely applied as an anti-oxidant, food additives, and bacterial growth. Moreover, it modulates enzymatic and non-enzymatic browning responses while protecting and storing food [1,2]. Conventional SO_3^{2-} with beverages are cider, alcoholic and non-alcoholic beer, wine, bottled fruit juices and concentrates. However, SO_3^{2-} damages to DNA and chromosomes, and is an uncertain allergen, so that a lot of people may be subjected to allergic reactions or even deadly asthma attacks. As stated by the Food and Drug Administration (FDA), inclusion of caution labels on all foodstuff and beverages containing more than 10 ppm of SO_3^{2-} with maximal concentrations of 50 mg L^{-1} in beer and 350 mg L^{-1} in wine shall be obligatory [3-5]. Hence, one of the prominent

* *Corresponding Author Email: h.beitollahi@yahoo.com*

aspects of food quality control and safety is to have a sulfite detection technique with more sensitivity, selectivity, and higher speed [6, 7].

Numerous techniques of sulfite determination exist such as ion-pair chromatography [8,9],high-performance liquid chromatography [10], flow injection analysis [11] and spectrophotometery method [12]. Yet, the techniques have usually defects (i.e., laborious, tiresome sample pre-treatment, expensiveness and in some cases lower level of sensitiveness and selectivities).

As a complementary choice, electro-chemical techniques measure the current responses produced by direct sulfite oxidation [13]. It has been confirmed that they are easy, cost-effective, and adjustable, have greater selectivities, and readily automated for routine analyses [14-18]. Nonetheless, sulfite behaves electrochemically poorly at typical solid electrode surfaces (glassy carbon, gold, & platinum), because numerous samples can be poisonous for the surfaces of electrode and decline sensitiveness and precision of the electrodes [19,20]. However, modifying the surface of electrodes significantly mitigates overpotentials and augments the electron transfer rates [21-26].

Appropriateness of determining minute concentrations analytes may additionally be increased rapidly via incorporation of nano-materials that significantly enhances surface area, electrical conductivity of electrodes, and performances. Recently, nano-material based electro-chemical sensors have been greatly attracted [27-36].There are different hopeful materials in nanotechnology; however, MoS_2nano-sheets gained a certain attention because of their specific electrical and physical features and simple syntheses. One of the mostly attended methods is Molybdenum disulphide (MoS_2) based nano-materials because of the related manifold useful properties. MoS_2 contains S-Mo-S triple layers of certain semi-conducting features of metal dichalcogenide compounds. Extraordinary electro-chemical and luminescence features emphasized on MoS_2 based nano-materials as new sensing probes in order to carefully detect a series of analytes. The respective multi dimensional structures have been the key reason for attention with their multi-faceted application potential. The ultrathin 2D MoS_2 layered structure exhibits higher surface area and generates a prominent supporting material to generate metallic nano-composites.

The charge transfer features of a composite can be enhanced by the synergic impact of metal nano-particles, including MoS_2 and tungsten nano-sheets [37-40].

Screen printed electrodes (SPEs) have functional applications as sensors for chemical analytes. They are advantageous for field analyses, including higher efficiency, little sample sizes, portable capacity and higher velocity. In addition, such SPEs are inexpensive, allowing them for disposability. In any case, such a characteristic is clearly important while testing biological samples. Therefore, they avoid surface fouling side effects [41-44].

This study showed the benefits of $MOWS_2$ nanocomposites for modifying a screen-printed electrode for examining the sulfite electro-chemical behaviors.

MATERIALS AND METHODS

Apparatus and chemicals

An Autolab potentiostat/galvanostat (PGSTAT 302N, Eco Chemie, the Netherlands) was applied for measuring electrochemicals. General Purpose Electrochemical System (GPES) software was employed to control conditions of experiments. The screen-printed electrode (DropSens, DRP-110, Spain) includes 3 main sections that contain a silver pseudo-reference electrode, a graphite working electrode, and graphite counter electrode. pH was measured by a Metrohm 710 pH meter.

Sulfite and all the remaining reagents had an analytical grade. They have been prepared via Merck (Darmstadt, Germany). Orthophosphoric acid and the related salts that were above the pH range of 2.0–9.0 were used for preparing the buffer solutions.

Hydrothermal synthesis of $MoWS_2$ nanocomposite

The following process was applied to produce $MoWS_2$. 3.85 mmol of $Na_2MoO_4{\cdot}2H_2O$ and 0.15 mmol of $Na_2WO_4{\cdot}2H_2O$ were dissolved in 40 mL of de-ionized water. In the next step, while continuously stirring the obtained aqueous solution was added with 15 mmol CH_4N_2S and 3 mmol $C_2H_2O_4.2H_2O$. As precursor solution was converted into a transparent liquid, it has been transported to a 60 mL Teflon liner, followed by loading in a stainless steel autoclave, heating at 200°C for 24 hours, repeatedly cleaning by distilled water and ethanol for removing impurities, and

finally vacuum-drying for 4 hours at 80 °C.

Preparation of the electrode

$MoWS_2$ nano-particles have been used to coat the bare screen-printed electrode. A stock solution of $MoWS_2$ nanoparticles in 1 mL of aqueous solution has been prepared by distributing 1 mg of $MoWS_2$ nano-particles via ultra-sonication for 30 minutes, whereas 5 µl of aliquots of the $MoWS_2$ suspension solution has been cast on carbon working electrodes. Then, we waited until the solvent evaporation at room temperature.

RESULTS AND DISCUSSION

Characterization

The FESEM images (MIRA3 TESCAN with EDX microanalysis) of the hydrothermally synthesized $MoWS_2$ composite is illustrated in Fig. 1, showing a 2 µm averaged diameter for each individual $MoWS_2$ flower-like microsphere. Densely stacked 2D curved nanopetals with 5 to 15-nm thickness were predominantly observed on the surface of this uniform spherical morphology. Therefore, these structures are called as ''$MoWS_2$ microflowers with nanopetals''. A crosswise and random way was found in such secondary structures, suggesting the ability of these heavily staggered 2D nanopetals to grow perpendicularly towards the surface and eventually to form the spherical shape. In conclusion, the synthesize of nanopetal-structured 3D hierarchical architecture can be observed obviously and definitely in accordance with the FESEM images prepared for the produced $MoWS_2$ composite.It can be said that the hydrothermal environment has completely affected $MoWS_2$ nanopetals in justifying the mechanism of producing the nanopetal structure. The primary duration of hydrothermal reaction at 200 °C caused a significant alteration in the structure of amorphous MoS_2/WS_2. These amorphous nanoparticles became spheroid with dense surface curls after descending trend from $Na_2MoO_4{\cdot}2H_2O$/ $Na_2WO_4{\cdot}2H_2O$ to MoS_2/WS_2, thereby eliminating the swinging links and lowering total energies. The spherical morphology can be formed for these primary structures spontaneously following the layered 2D characteristic of MoS_2/WS_2. The structure of composite may be in the form of curls in the hydrothermal environment because of completely matched lattice constants of MoS_2 and WS_2, thereby driving the confined growth of such hierarchical structure without remarkable alteration.

The EDX spectra prepared for the layers verify the existence of Mo, W and S in $MoWS_2$ with no additional impurities of the source ingredients, as shown in Fig. 2.

The XRD pattern prepared from the synthesized $MoWS_2$ composite structure is shown in Fig. 3. The distinct sharp diffraction peaks for the $MoWS_2$ composite means a high level of crystallinity regarding such hydrothermally fabricated samples. The distinct sharp diffraction peaks for the composite also means a higher level of crystallinity regarding such hydrothermally fabricated samples. The standard XRD peaks at 14.38° and 14.32°, respectively, show (002) reflections of MoS_2 and WS_2. Joint Committee on Powder Diffraction Standards (JCPDS=37-1492) card was implemented to index the X-ray diffraction pattern. Based on the Bragg's equation, $2d \sin \theta = n\lambda$, so that d represents inter-planar spacing, θ is diffraction angle, n is diffraction series, and λ indicates X-ray wavelengths. Standard values are slightly higher than those of all peaks of diffraction (002) calculated for such species, and this demonstrates that the interlayer spacing is larger and a strain exists between layers for curve hierarchical structure of the fabricated specimens.

Electrochemical behaviour of sulfite at the surface of different electrodes

The electrochemical behaviour of sulfite depends on the pH value of the aqueous solution. Thus, it is essential to optimize the solution pH in order to gain more useful results for electro-oxidation of sulfite. Therefore, sulfite electrochemical behaviour was examined in 0.1 M PBS at distinct pH numbers (2.0–9.0) at $MOWS_2$/ SPE surface by voltammetry. The results indicated more advantagousness of neutral conditions for sulfite electro-oxidation at $MOWS_2$/SPE surface in comparison to the basic or acidic medium. Here, pH 7.0 was selected as an optimal pH for sulfite electro-oxidation at $MOWS_2$/SPE surface.

Fig. 4 shows responses of CV to electro-oxidation of 100.0 µM Sulfite at the unmodified SPE (curve a) and $MOWS_2$/SPE (curve b). The peak potential occurs at 660 mV due to sulfite oxidation, which is around 160 mV more negative than the unchanged SPE. Furthermore, $MOWS_2$/ SPE exhibits very high anodic peak currents for sulfite oxidation than that of the unchanged SPE. This showed a significant improvement of the

Fig. 1. FESEM Image of $MoWS_2$ composite.

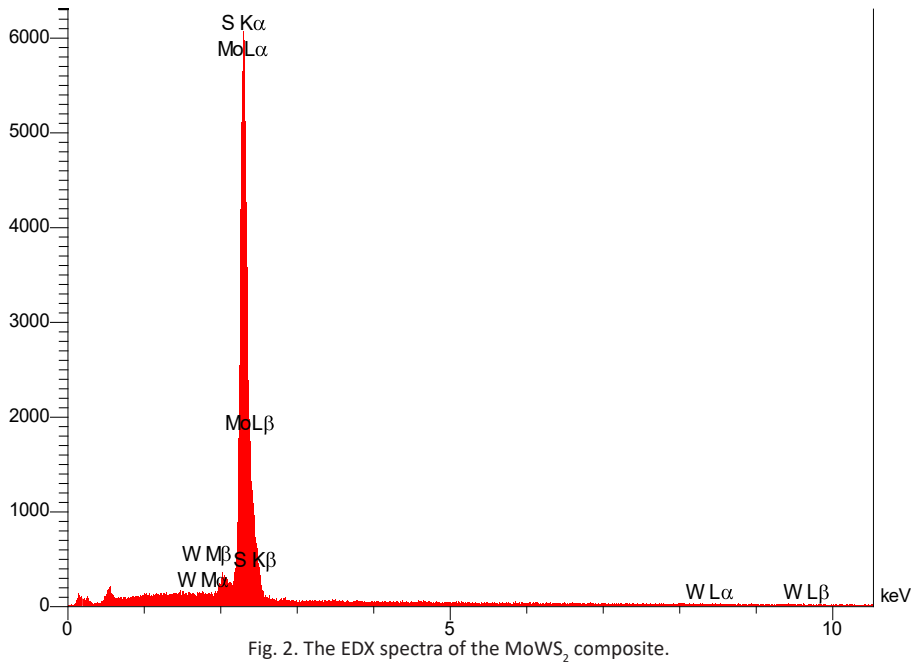

Fig. 2. The EDX spectra of the $MoWS_2$ composite.

electrode performance toward sulfite oxidation by changing the constant SPE with $MOWS_2$ nanocomposite.

Impact of scan rate

Researchers investigated the impact of the rates of potential scan on sulfite oxidation current (Fig.

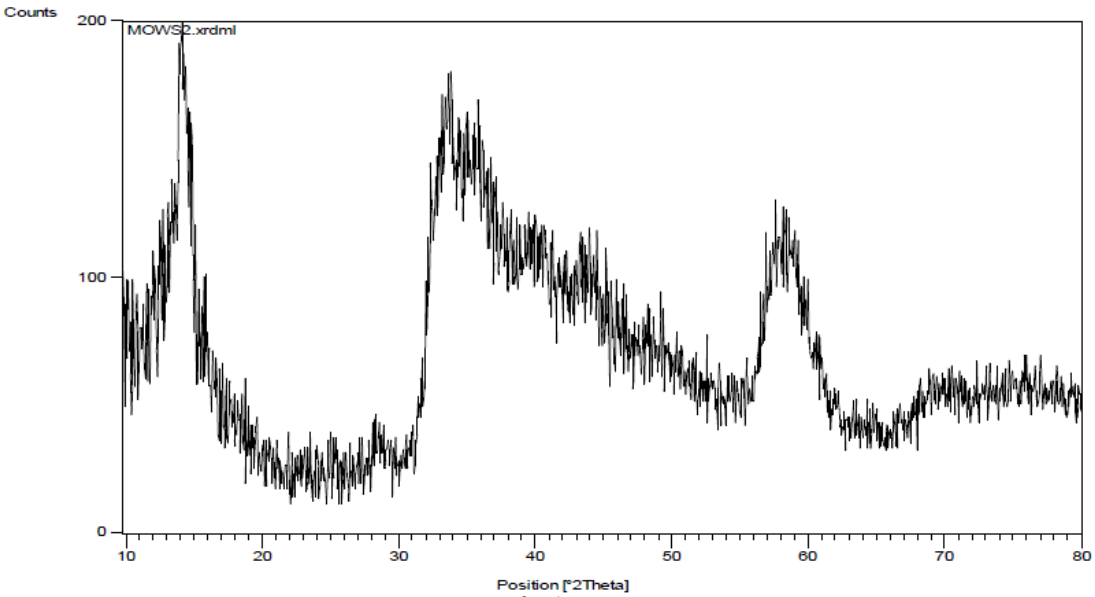

Fig. 3. XRD patterns for the $MoWS_2$ composite.

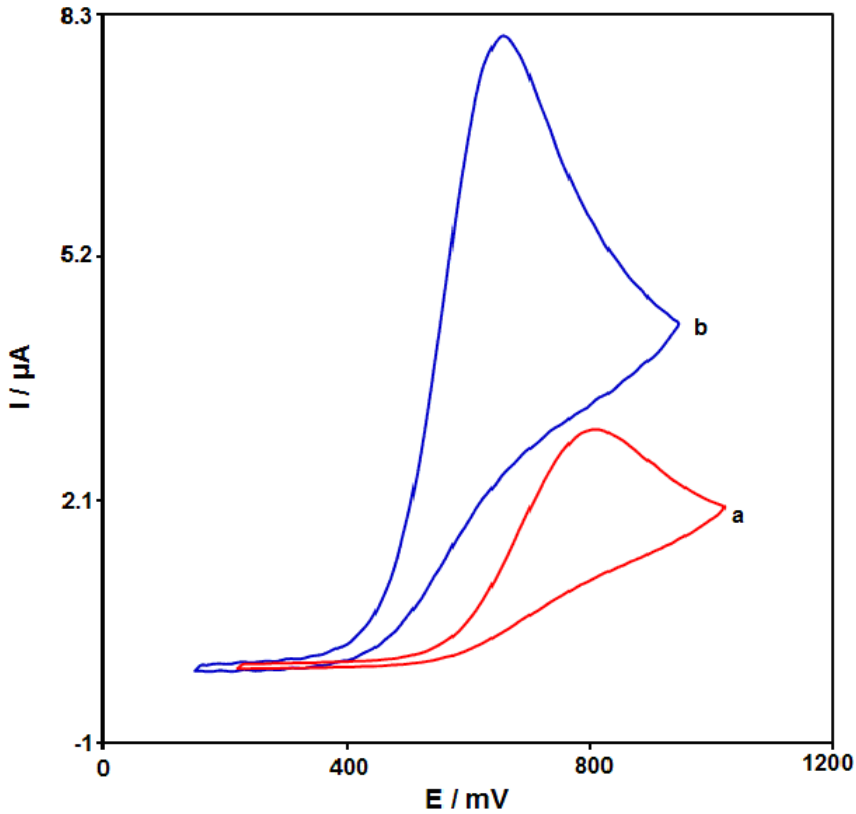

Fig.4. CVs of a) SPE and b) $MOWS_2$ /SPE in the presence of 100.0 µM of sulfite at pH 7.0. Rate of scan in all cases was found to be 50 mV s^{-1}.

5). Findings indicated induction of enhancement in the current of the peak by the increased potential scan rate. Additionally, diffusion in oxidation processes are monitored, as inferred by the linear

dependence of the anodic peak current (Ip) on the square root of the potential scan rate ($v^{1/2}$) for sulfite [45-47].

Chronoamperometric measurements

Chronoamperometric measurements of sulfite at $MOWS_2$/SPE were conducted by adjusting the working electrode potential at 0.71 V for different concentrations of sulfite (Fig. 6) in PBS (pH 7.0), respectively. For electroactive materials (sulfite in this case) with a diffusion coefficient of D, the Cottrell equation describes current seen for electrochemical reaction at the mass transport limited condition:

$$I = nFAD^{1/2}C_b\pi^{-1/2}t^{-1/2} \quad (1)$$

where D and C_b respectively represent diffusion coefficient ($cm^2\ s^{-1}$) and bulk concentration (mol cm^{-3}). Experimental plots of I versus $t^{-1/2}$ were used with the best fits for various concentrations of sulfite (Fig. 6A). Then, the resultant straight lines slopes were drawn against sulfite concentrations (Fig. 6B). According to the resultant slope and the Cottrell equation, mean values of D was 8.4×10^{-6} cm^2/s for sulfite.

Calibration plots and detection limits

The electro-oxidation peak currents of sulfite at $MOWS_2$/SPE surface can be applied to define sulfite in the solution. Since the increased sensitivity and more suitable properties for analytical utilizations are considered as the benefits of differential pulse voltammetry (DPV), $MOWS_2$/SPE in 0.1 M PBS consisting of different distinct concentrations of sulfite was used to conduct DPV experiments (Fig. 7). It was found that the electrocatalytic peak currents of sulfite oxidation at $MOWS_2$/SPE surface linearly depended on sulfite concentrations above the range of 0.08 to 700.0 µM (with a correlation coefficient of 0.9997), while determination limit (3σ) was achieved to be 0.02 µM.These values are comparable with values reported by other research groups for the determination of sulfiteat

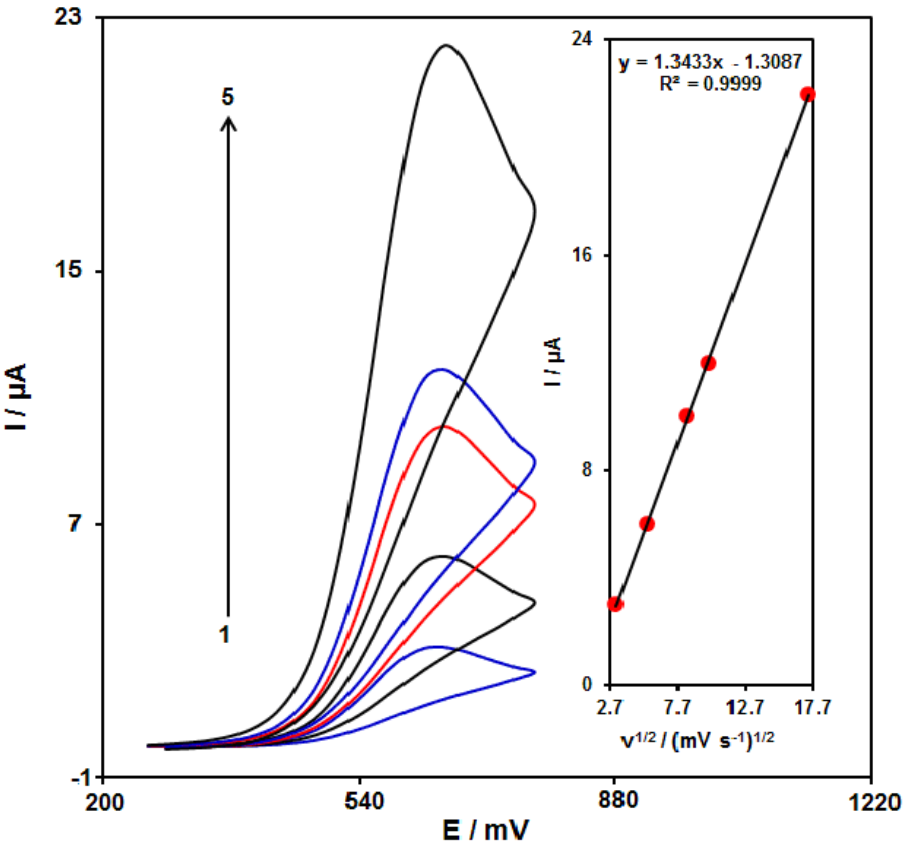

Fig. 5. CVs of $MOWS_2$/SPE in 0.1 M PBS (pH 7.0) consisting of 100.0 µM of sulfite at different scan rates. Values 1–5 are in agreement with 10, 30, 70, 100 and 300 mV s^{-1}.

the surface of modified electrodes (see Table 1).

Stability and repeatability of $MOWS_2$/SPE

Testing stability of $MOWS_2$/SPE has been done by maintaining the suggested sensor at pH=7.0 in PBS for 15 days and then recording cyclic voltammogram of the solution containing 70.0 µM of sulfite for comparison with cyclic voltammogram obtained before immersion. Oxidation peak of sulfite has not modified, and the current showed a less than 2.7 % decline in signals in comparison to the initial response, which suggests that $MOWS_2$/SPE have good stability.

Examining the anti-fouling characteristic of the modified SPE towards sulfite oxidation and the respective products have been performed by cyclic voltammetry for the modified SPE before and after using in the presence of sulfite. Recording the cyclic voltammograms have been done in the presence of sulfite after cycling the potential fifteen times at a 50 mV s^{-1}. The currents declined by less than 2.2%, and the peak potential has not altered.

Interference study

The effects of different materials that can have interference with the 50.0 µM sulfite detection, including biological fluids and pharmaceuticals, were evaluated at the optimal conditions. The maximum level of the interfering materials with error of <±5% for the sulfite detection was regarded as the tolerance limit. These materials were L -lysine, S^{2-}, glucose, Fe^{+3}, NH_4^+, sucrose, Mg^{2+}, fructose, hydroxylamine, hydrazine, lactose, benzoic acid, Al^{3+}, ascorbic acid, F^-, SO_4^{2-}, and sucrose, which exhibited no interference in the sulfite detection.

Analyzing real sample

The method illustrated above was used to evaluate $MOWS_2$/SPE usability for determining sulfite in real samples in order to determine sulfite

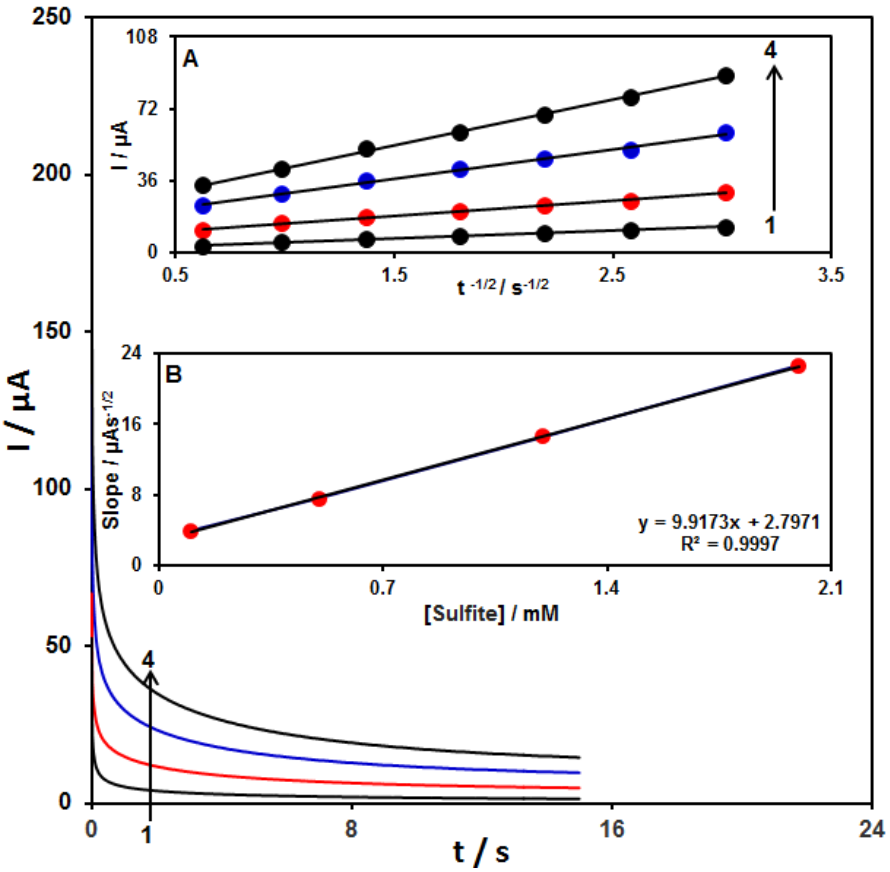

Fig. 6. Chronoamperograms gained at $MOWS_2$/SPE in 0.1 M PBS (pH 7.0) for various concentrations of sulfite. Values 1–4 are in agreement with 0.1, 0.5, 1.2 and 2.0 mM of sulfite. Insets: (A) Plots of I versus $t^{-1/2}$ achieved from chronoamperograms 1–4. (B) The slope plot of the straight lines against sulfite concentrations.

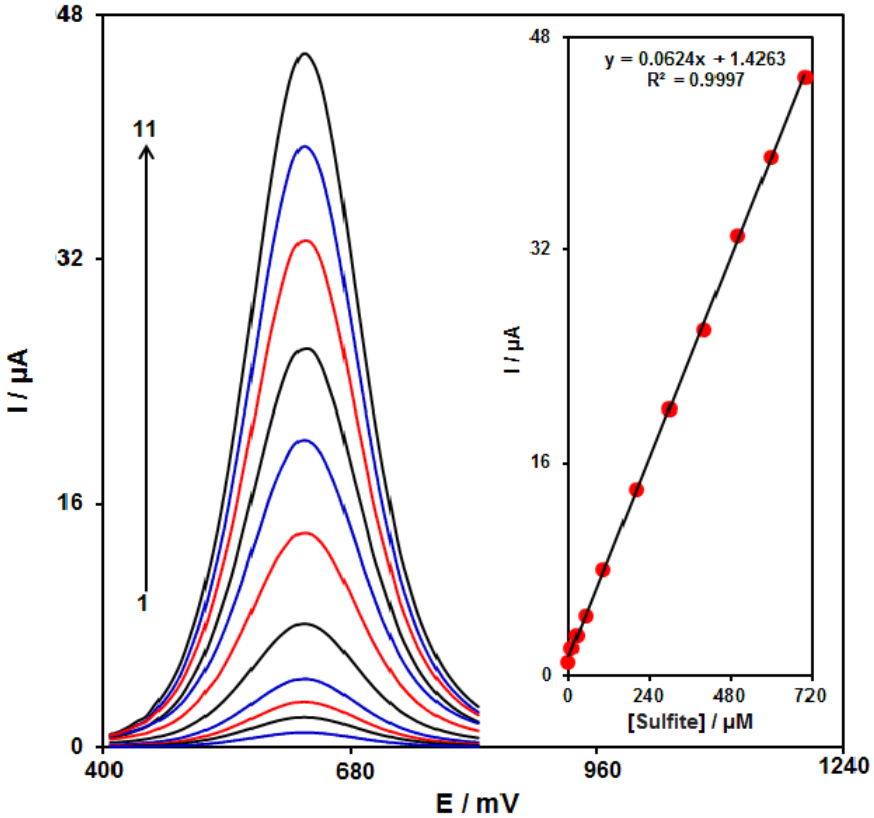

Fig. 7. DPVs of $MOWS_2$/SPE in 0.1 M PBS (pH 7.0) composing of various concentrations of sulfite. Values 1–11 are in agreement with 0.08, 5.0, 25.0, 50.0, 100.0, 200.0, 300.0, 400.0, 500.0, 600.0 and 700.0 µM of sulfite. The inset shows the peak current plot as a concentration function of sulfite within the range of 0.08 to 700.0 µM.

Table 1. Performance comparison of electrochemical sensors for determination of sulfite.

Methods	Electrochemical Sensors	Linear Range	Limit of Detection	Reference
Square wave voltammetry	MWCNT/CPE	25.0–500 µM	16 µM	49
Differential pulse voltammetry	2,7- BFEFMCPE/CPE	4.0– 4430µM	0.21µM	50
Amperometry	Cu-salen polymer/Pt	4.0 – 69.0 µM	1.2 µM	51
Differential pulse voltammetry	BFCNPEs	0.1-400 µM	0.09 µM	52
Amperometry	RuOHCF/GCE	50 - 500 µM	20 µM	53
Amperometry	AuNPs /SPCE	9.80-83.33µM	9.8 µM	54
Amperometry	OMC/NiHCF/Au	2.5–50000 ìM	2.5 ìM	55
Cyclic voltammetry	AFc/CB/PVB/GCE	30–4000 ìM	15 ìM	56
Amperometry	MWCNT/CHITFC/ GCE	5–1500 ìM	2.8 ìM	57
Differential pulse voltammetry	$MOWS_2$/SPE	0.08-700.0µM	0.02 µM	This Work

[a]Multiwall Carbon Nanotubes (MWCNT); [b]2,7-bis (ferrocenyl ethyl) fluoren-9-one (2, 7-BFEFMCPE); [c]Benzoylferrocene and carbon nanotube (BFCNPE); [d]Ruthenium-oxidehexacyanoferrate (RuOHCF); [e]Gold nanoparticles (AuNPs); [f]Nickelhexacyanoferrate (NiHCF) ordered mesoporous carbon covering on a gold electrode surface (NiHCF/OMC/Au); [g]Acetylferrocene–carbon Black–Poly(vinyl butyral), (AFc/CB/PVB); [h]Multiwalled carbon nanotubes (MWCNTs)/ferrocene-branched chitosan (CHIT-Fc)

Table 2. Determining sulfite in real samples through $MOWS_2$/SPE. All the concentrations are in µM (n=3).

Sample	Spiked	Found	Recovery (%)	R.S.D. (%)
	0	-	-	-
Well water	7.0	6.9	98.6	2.4
	12.0	12.3	102.5	1.9
	17.0	16.9	99.4	3.4
	22.0	22.2	100.9	2.3
	0	-	-	-
River water	5.0	5.1	102	3.2
	15.0	14.8	98.7	1.8
	25.0	24.8	99.2	2.9
	35.0	35.5	101.4	2.5

in river water and well water samples. Therefore, the standard addition technique was applied. Table 2 reports the results. Acceptable recoveries of sulfite were observed, and reproducible results were shown with regard to the mean relative standard deviation (R.S.D.).

CONCLUSION

The present research examined electro-chemical oxidation behaviors of sulfite at $MOWS_2$/SPE. The research findings indicated facilitation of electro-chemical responses of sulfite via $MOWS_2$ because of its great surface area, higher absorptive capacity, and very good catalytic ability. Additionally, it is effortless and uncomplicated to be fabricated. The peak current exhibited acceptable linear relationship with sulfite concentrations between 0.08 to 700.0 µM. Determination limit of sulfite has been found to be 0.02 µM. Functional features of the proposed sensor (e.g., acceptable stability and reproducible capacity) are a promising fact, indicating that it can be applied as an influential device to determine the sulfite in real samples.

ACKNOWLEDGEMENTS

The authors acknowledge the financial support provided for this project (Project No. 9800552 and ethics code 1398.365) by the Kerman University of Medical Sciences, Kerman, Iran.

CONFLICT OF INTERESTS

The authors declare that there is no conflict of interests regarding the publication of this paper.

REFERENCES

1. Wang R, Mao Y, Qu H, Chen W, Ma A, Zheng L. Highly sensitive and selective sulfite sensors based on solution-gated graphene transistors with multi-walled carbon nanotube functionalized gate electrodes. Food Chem. 2019;290:101-106.
2. Li D, Tian X, Li Z, Zhang J, Yang X. Preparation of a Near-Infrared Fluorescent Probe Based on IR-780 for Highly Selective and Sensitive Detection of Bisulfite–Sulfite in Food, Living Cells, and Mice. J Agric Food Chem. 2019;67(10):3062-3067.
3. Pandi K, Sivakumar M, Chen S-M, Sakthivel M, Raghavi G, Chen T-W, et al. Electrochemical Synthesis of Lutetium (III) Hexacyanoferrate/poly(taurine) Modified Glassy Carbon Electrode for the Sensitive Detection of Sulfite in Tap Water. J Electrochem Soc. 2018;165(10):B469-B474.
4. Manikandan VS, Liu Z, Chen A. Simultaneous detection of hydrazine, sulfite, and nitrite based on a nanoporous gold microelectrode. J Electroanal Chem. 2018;819:524-532.
5. Wu Z, Guo F, Huang L, Wang L. Electrochemical nonenzymatic sensor based on cetyltrimethylammonium bromide and chitosan functionalized carbon nanotube modified glassy carbon electrode for the determination of hydroxymethanesulfinate in the presence of sulfite in foods. Food Chem. 2018;259:213-218.
6. Jirimali HD, Nagarale RK, Saravanakumar D, Shin W. Ferrocene Tethered Polyvinyl Alcohol/Silica Film Electrode for Electrocatalytic Sulfite Sensing. Electroanalysis. 2018;30(5):828-833.
7. do Carmo DR, Maraldi VA, Cumba LR. Voltammetric Properties of Nickel Hexacyanoferrate (III) Obtained on the Titanium (IV) Silsesquioxane Occluded into the H-FAU Zeolite for Detection of Sulfite. Silicon. 2018;11(1):267-276.
8. Steudel R, Münchow V. Sulphur compounds. J Chromatogr. 1992;623(1):174-177.
9. Zuo Y, Chen H. Simultaneous determination of sulfite, sulfate, and hydroxymethanesulfonate in atmospheric waters by ion-pair HPLC technique. Talanta. 2003;59(5):875-881.
10. McFeeters RF, Barish AO. Sulfite Analysis of Fruits and Vegetables by High-Performance Liquid Chromatography (HPLC) with Ultraviolet Spectrophotometric Detection. J Agric Food Chem. 2003;51(6):1513-1517.
11. Su X, Wei W. Flow injection determination of sulfite in wines and fruit juices by using a bulk acoustic wave impedance sensor coupled to a membrane separation technique. The Analyst. 1998;123(2):221-224.

12. Yuan W, Xiang B, Yu L, Xu J. A Non-invasive Method for Screening Sodium Hydroxymethanesulfonate in Wheat Flour by Near-Infrared Spectroscopy. Food Analytical Methods. 2011;4(4):550-558.
13. Ensafi A A. Karimi-Maleh H, Ferrocenedicarboxylic Acid Modified Multiwall Carbon Nanotubes Paste Electrode for Voltammetric Determination of Sulfite, International Journal of Electrochemical Science. 2010;5:392– 406.
14. Beitollai H, Garkani-Nejad F, Tajik S, Jahani S, Biparva P. Voltammetric determination of amitriptyline based on graphite screen printed electrode modified with a Copper Oxide nanoparticles. International Journal of Nano Dimension. 2017;8:197-205.
15. Lee SM, Zirlianngura, Anjudikkal J, Tiwari D. Electrochemical sensor for trace determination of cadmium(II) from aqueous solutions: use of hybrid materials precursors to natural clays. Int J Environ Anal Chem. 2016;96(5):490-504.
16. Reza Ganjali M. Highly Sensitive Determination of Theophylline Based on Graphene Quantum Dots Modified Electrode. International Journal of Electrochemical Science. 2018:2448-2461.
17. Tcheumi HL, Babu BR. Surfactant-intercalated smectite modified electrode: sensitive electrochemical detection of methyl orange dye. Int J Environ Anal Chem. 2017;97(13):1207-1222.
18. Kazemipour M, Ansari M, Mohammadi A, Beitollahi H, Ahmadi R. Use of adsorptive square-wave anodic stripping voltammetry at carbon paste electrode for the determination of amlodipine besylate in pharmaceutical preparations. J Anal Chem. 2009;64(1):65-70.
19. Yin H, Zhou Y, Ai S, Ma Q, Zhu L, Lu L. Electrochemical oxidation determination and voltammetric behaviour of 4-nitrophenol based on Cu_2O nanoparticles modified glassy carbon electrode. Int J Environ Anal Chem. 2012;92(6):742-754.
20. Jiang YN, Luo HQ, Li NB. Determination of nitrite with a nano-gold modified glassy carbon electrode by cyclic voltammetry. Int J Environ Anal Chem. 2007;87(4):295-306.
21. Beitollahi H, Tajik S, Asadi MH, Biparva P. Application of a modified graphene nanosheet paste electrode for voltammetric determination of methyldopa in urine and pharmaceutical formulation. Journal of Analytical Science and Technology. 2014;5(1).
22. Karimi-Maleh H, Fakude CT, Mabuba N, Peleyeju GM, Arotiba OA. The determination of 2-phenylphenol in the presence of 4-chlorophenol using nano-Fe_3O_4/ionic liquid paste electrode as an electrochemical sensor. J Colloid Interface Sci. 2019;554:603-610.
23. Karimi-Maleh H, Sheikhshoaie M, Sheikhshoaie I, Ranjbar M, Alizadeh J, Maxakato NW, et al. A novel electrochemical epinine sensor using amplified CuO nanoparticles and a n-hexyl-3-methylimidazolium hexafluorophosphate electrode. New J Chem. 2019;43(5):2362-2367.
24. Tahernejad-Javazmi F, Shabani-Nooshabadi M, Karimi-Maleh H. 3D reduced graphene oxide/$FeNi_3$-ionic liquid nanocomposite modified sensor; an electrical synergic effect for development of tert-butylhydroquinone and folic acid sensor. Composites Part B: Engineering. 2019;172:666-670.
25. Khodadadi A, Faghih-Mirzaei E, Karimi-Maleh H, Abbaspourrad A, Agarwal S, Gupta VK. A new epirubicin biosensor based on amplifying DNA interactions with polypyrrole and nitrogen-doped reduced graphene: Experimental and docking theoretical investigations. Sensors Actuators B: Chem. 2019;284:568-574.
26. Miraki M, Karimi-Maleh H, Taher MA, Cheraghi S, Karimi F, Agarwal S, et al. Voltammetric amplified platform based on ionic liquid/NiO nanocomposite for determination of benserazide and levodopa. J Mol Liq. 2019;278:672-676.
27. Mazloum-Ardakani M, Beitollahi H, Amini MK, Mirkhalaf F, Mirjalili B-F, Akbari A. Application of 2-(3,4-dihydroxyphenyl)-1,3-dithialone self-assembled monolayer on gold electrode as a nanosensor for electrocatalytic determination of dopamine and uric acid. The Analyst. 2011;136(9):1965.
28. Muzvidziwa T, Moyo M, Okonkwo JO, Shumba M, Nharingo T, Guyo U. Electrodeposition of zinc oxide nanoparticles on multiwalled carbon nanotube-modified electrode for determination of caffeine in wastewater effluent. Int J Environ Anal Chem. 2017;97(7):623-636.
29. Soltani H, Beitollahi H, Hatefi-Mehrjardi AH, Tajik S, Torkzadeh-Mahani M. Voltammetric determination of glutathione using a modified single walled carbon nanotubes paste electrode. Analytival and BioanalyticalElectrochemistry.2014;6(1):67-79.
30. Qi-mei LUO, Deng-you LIU, Hui-xian WANG, Hua ZHOU, Dong ZHOU. Electrochemical determinnation of catechol with nano-gold/carbon nanotubes modified graphite electrode [J]. China Environmental Science.2010;10.
31. Sun X, Zhu Y, Wang X. Amperometric Immunosensor Based on a Protein A/Deposited Gold Nanocrystals Modified Electrode for Carbofuran Detection. Sensors. 2011;11(12):11679-11691.
32. Mehdi Motaghi M. Nanostructure Electrochemical Sensor for Voltammetric Determination of Vitamin C in the Presence of Vitamin B6: Application to Real Sample Analysis. International Journal of Electrochemical Science. 2016:7849-7860.
33. Khoobi A, Attaran AM, Yousofi M, Enhessari M. A sensitive lead titanate nano-structured sensor for electrochemical determination of pentoxifylline drug in real samples. Journal of Nanostructure in Chemistry. 2019;9(1):29-37.
34. Moghaddam HM, Beitollahi H, Tajik S, Malakootian M, Maleh HK. Simultaneous determination of hydroxylamine and phenol using a nanostructure-based electrochemical sensor. Environ Monit Assess. 2014;186(11):7431-7441.
35. El-Shal MA, Hendawy HAMH, Eldin GMG, El-Sherif ZA. Application of nano graphene-modified electrode as an electrochemical sensor for determination of tapentadol in the presence of paracetamol. Journal of the Iranian Chemical Society. 2019;16(5):1123-1130.
36. Alshahrani LA, Liu L, Sathishkumar P, Nan J, Gu FL. Copper oxide and carbon nano-fragments modified glassy carbon electrode as selective electrochemical sensor for simultaneous determination of catechol and hydroquinone in real-life water samples. J Electroanal Chem. 2018;815:68-75.
37. Barua S, Dutta HS, Gogoi S, Devi R, Khan R. Nanostructured MoS2-Based Advanced Biosensors: A Review. ACS Applied Nano Materials. 2017;1(1):2-25.
38. Tuteja SK, Duffield T, Neethirajan S. Liquid exfoliation of 2D MoS_2 nanosheets and their utilization as a label-free electrochemical immunoassay for subclinical ketosis. Nanoscale. 2017;9(30):10886-10896.
39. Devi R, Gogoi S, Barua S, Sankar Dutta H, Bordoloi M, Khan

R. Electrochemical detection of monosodium glutamate in foodstuffs based on Au@MoS_2/chitosan modified glassy carbon electrode. Food Chem. 2019;276:350-357.
40. Beitollahi H, Dourandish Z, Tajik S, Ganjali MR, Norouzi P, Faridbod F. Application of graphite screen printed electrode modified with dysprosium tungstate nanoparticles in voltammetric determination of epinephrine in the presence of acetylcholine. Journal of Rare Earths. 2018;36(7):750-757.
41. Silva RdO, da Silva ÉA, Fiorucci AR, Ferreira VS. Electrochemically activated multi-walled carbon nanotubes modified screen-printed electrode for voltammetric determination of sulfentrazone. J Electroanal Chem. 2019;835:220-226.
42. Taherkhani A, Jamali T, Hadadzadeh H, Karimi-Maleh H, Beitollahi H, Taghavi M, et al. ZnO nanoparticle-modified ionic liquid-carbon paste electrodefor voltammetric determination of folic acid in food and pharmaceutical samples. Ionics. 2013;20(3):421-429.
43. Zhang Y, Jiang X, Zhang J, Zhang H, Li Y. Simultaneous voltammetric determination of acetaminophen and isoniazid using MXene modified screen-printed electrode. Biosensors Bioelectron. 2019;130:315-321.
44. Mohtar LG, Aranda P, Messina GA, Nazareno MA, Pereira SV, Raba J, et al. Amperometric biosensor based on laccase immobilized onto a nanostructured screen-printed electrode for determination of polyphenols in propolis. Microchem J. 2019;144:13-18.
45. Bijad M, Karimi-Maleh H, Farsi M, Shahidi S-A. An electrochemical-amplified-platform based on the nanostructure voltammetric sensor for the determination of carmoisine in the presence of tartrazine in dried fruit and soft drink samples. Journal of Food Measurement and Characterization. 2017;12(1):634-640.
46. Jamali T, Karimi-Maleh H, Khalilzadeh MA. A novel nanosensor based on Pt:Co nanoalloy ionic liquid carbon paste electrode for voltammetric determination of vitamin B9 in food samples. LWT - Food Science and Technology. 2014;57(2):679-685.
47. Cheraghi S, Taher MA, Karimi-Maleh H. Highly sensitive square wave voltammetric sensor employing CdO/SWCNTs and room temperature ionic liquid for analysis of vanillin and folic acid in food samples. J Food Compost Anal. 2017;62:254-259.